Orbital Interactions between a C_{60} Molecule and Cu(111) Surface

Atsushi Ogawa,[†] Masamitsu Tachibana,[†,‡] Masakazu Kondo,[‡] Kazunari Yoshizawa,*[,‡] Hiroshi Fujimoto,*[,†] and Roald Hoffmann*[,§]

Department of Molecular Engineering, Kyoto University, Kyoto 606-8501, Japan, Institute for Materials Chemistry and Engineering, Kyushu University, Fukuoka 812-8581, Japan, Department of Chemistry and Chemical Biology, Cornell University, Ithaca, New York 14853-1301

Received: March 10, 2003; In Final Form: August 25, 2003

C−Cu orbital interactions between a two-layer Cu_{10} or three-layer Cu_{34} cluster model of a Cu(111) surface and an adsorbed single C_{60} molecule have been theoretically investigated, so as to elucidate the nature of the C_{60}−Cu(111) bonding and orientational configuration of the C_{60} molecule on a Cu surface. Geometry optimizations and single-point calculations at the B3LYP/LanL2MB level of theory and fragment molecular orbital (FMO) analyses, coupled with a paired-interaction-orbital (PIO) scheme at the extended Hückel level of theory, have been performed for five symmetric adsorption models, in which a C_{60} molecule is attached to the Cu_{10} or Cu_{34} cluster respectively by a six-membered ring (6-ring), by a five-membered ring (5-ring), by a C−C bond belonging to two 6-rings (6−6 bond), by a C−C bond belonging to a 6-ring and a 5-ring (5−6 bond), and by an edge carbon atom that is located at the center of two 6-rings and a 5-ring. Large stabilization is obtained for adsorption by an edge carbon atom or a 6−6 bond, whereas the other coordination types are not favored. Our result differs from an XPD experimental result for a C_{60} monolayer on Cu(111), in which adsorption by a 6-ring is most favored. The discrepancy strongly suggests that C_{60}−C_{60} interactions contribute significantly to the determination of C_{60} orientations in C_{60}/Cu(111) monolayer systems.

Introduction

Structures of fullerene-adsorbed surfaces (Cu,[1−3] Al,[1] Pt,[4,5] Ni,[2,4,6] Au,[7−9] Pd,[10,11] Ag,[12,13] Si,[14−16] and so on) have been extensively studied by several experimental methods, e.g., scanning tunneling microscopy (STM), low energy electron diffraction (LEED), X-ray photoelectron spectroscopy (XPS), X-ray photoelectron diffraction (XPD), and so on. In particular, binding and orientations of adsorbed C_{60} molecules on various surfaces have attracted much attention in recent years. Fasel et al. first determined the orientation of adsorbed C_{60} molecules on a Cu(111) surface by the use of XPD and single-scattering cluster (SSC) calculations.[1] Since then, a variety of C_{60} orientations on different surfaces have been observed and characterized by a combination of XPD and SSC calculations.[1,3,11,13] For example, it has been reported that C_{60} is bound by a six-membered ring on Cu(111) and Al(111),[1] by an edge carbon atom on Al(001), and by a bond common to a five-membered ring and a six-membered ring (5−6 bond) on Cu(110) and Ni(110).[1,3] Several different C_{60} orientations were found at the same time on Ag(001)[13] and some semiconductor surfaces such as Si(111).[15]

Two main factors, namely, C_{60}−surface and C_{60}−C_{60} interactions, are considered to be important in determining the orientations of C_{60} on substrates. In the experimental studies mentioned above, C_{60} molecules form a monolayer, and therefore C_{60}−C_{60} van der Waals interactions should play an important role in determining the orientation of C_{60}. Indeed, some experimental results showed the significance of C_{60}−C_{60} interactions in C_{60} monolayer systems.[3] C_{60}−C_{60} interactions have been studied theoretically[17,18] by Nakamura et al., who demonstrated a correlation between the band gap and C_{60}−C_{60} distance in the C_{60} monolayers.[18] The precise nature of local C_{60}−surface interactions has not yet been clarified[19] despite many studies on C_{60} monolayers.[1,20] Thus, the theoretical analysis of interactions between a metal surface and an adsorbed C_{60} molecule is of great interest and indispensable for a better understanding of the adsorption mode and binding of C_{60} on many kinds of surfaces. Studies on C_{60}−surface interactions will also be helpful in interpreting such experimental results as an STM study by Tang et al., in which they studied a single C_{60} molecule rolling on Cu surfaces.[21]

By performing a fragment molecular orbital (FMO) analysis coupled with a paired-interaction-orbital (PIO) scheme, some of the present authors have studied orbital interactions between C_{60} and transition metal complexes.[22] Very recently, we reported a theoretical study on the nature of the S−Au(111) bonding in the organosulfur/Au(111) self-assembled monolayer systems using the same method.[23] In this study, we apply this method to clarify the essence of the interaction between a single C_{60} molecule and Cu(111) surface.

Cluster Models and Geometry Optimizations. The Cu(111) surface is stable against external perturbation and adsorbs C_{60} molecules without reconstruction.[1,7−9] To determine possible orientations of C_{60} molecules on a Cu(111) surface, we considered five adsorption models in which a C_{60} molecule is attached to a two-layer Cu_{10} cluster by a six-membered ring (6-ring), by a five-membered ring (5-ring), by a C−C bond belonging to two 6-rings (6−6 bond), by a C−C bond shared by a 6-ring and a 5-ring (5−6 bond), and by an edge carbon atom located at the center of two 6-rings and a 5-ring, as

* To whom correspondence should be addressed. E-mail: kazunari@ms.ifoc.kyushu-u.ac.jp (K.Y.); lavender@zeus.eonet.ne.jp (H.F.); rh34@cornell.edu (R.H.).
† Kyoto University.
‡ Kyushu University.
§ Cornell University.

10.1021/jp0303220 CCC: $25.00
Published on Web 10/25/2003

SCHEME 1

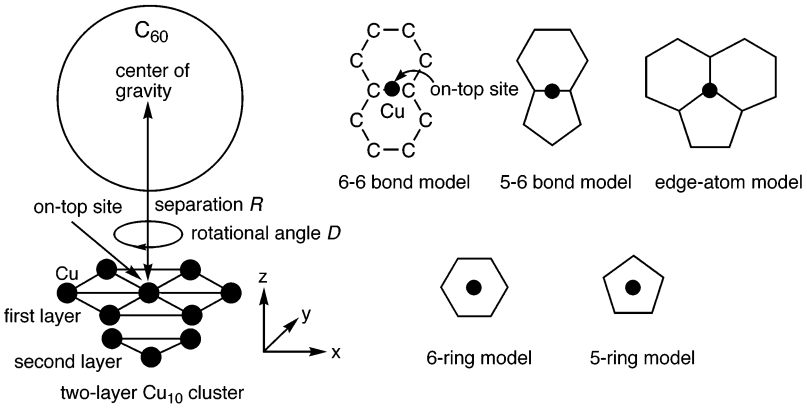

SCHEME 2

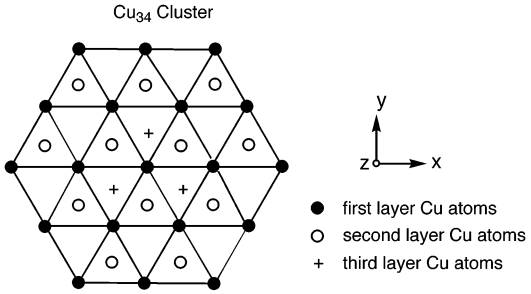

illustrated in Scheme 1. We label these models 6-ring model, 5-ring model, 6−6 bond model, 5−6 bond model, and edge-atom model, respectively. In these models, we assumed that a C_{60} molecule is located on the on-top site, that is, the center of gravity of the C_{60} part is just above the central Cu atom of the first Cu layer of the Cu_{10} cluster.[1,24] We first optimized the structure of a C_{60} molecule under I_h symmetry at the B3LYP[25]/LanL2MB[26] level of theory. All of the B3LYP/LanL2MB calculations in this work were performed using the Gaussian98 program package.[27]

Optimized lengths of the 6−6 and 5−6 bonds are, respectively, 1.41 and 1.48 Å, consistent with results of an NMR (1.40 and 1.46 Å, respectively)[28] and an X-ray (1.40 and 1.45 Å, respectively)[29] experiments. The geometry of the C_{60} part is fixed in this I_h structure in geometry optimizations of the five adsorption models.[30] The distance between the adjacent Cu atoms in the Cu_{10} cluster is fixed to be 2.56 Å, the value for bulk Cu. Then, for each of the five adsorption models, we optimized at the B3LYP/LanL2MB level the separation R between the center of gravity of the C_{60} sphere and the central Cu atom of the first layer of the Cu_{10} cluster, and the rotational angle D of the C_{60} part around the surface normal that penetrates the center of the Cu layers (z axis), as shown in Scheme 1. We calculated the heats of adsorption of a C_{60} molecule by subtracting the computed total energies of the Cu_{10} cluster ($E(Cu_{10})$) and the optimized C_{60} molecule ($E(C_{60})$) from that of an optimized C_{60}−Cu_{10} system ($E(C_{60} + Cu_{10})$). Mulliken populations were also calculated for the five adsorption models.

Next we attached 24 Cu atoms to the optimized C_{60}−Cu_{10} models, in which the Cu−Cu distance is 2.56 Å, to investigate interactions over a wider surface area. In the five C_{60}−Cu_{34} models thus constructed, a C_{60} molecule is attached to a three-layer Cu_{34} cluster, as illustrated in Scheme 2. As in the C_{60}−Cu_{10} models, we calculated the heats of adsorption of a C_{60} molecule and the Mulliken charges for the C_{60}−Cu_{34} systems by performing B3LYP/LanL2MB single-point calculations.

Results and Discussion

Adsorption of C_{60} on a Cu(111) Surface. We show in Figure 1 optimized structures of the C_{60}−Cu_{10} models and the nearest C−Cu distances. For the 6-ring model, our calculation gave a structure with the azimuthal orientation different from the result of an XPD experiment by 30°, although we started the B3LYP/LanL2MB geometry optimization from a structure in which the C_{60} molecule is oriented with respect to the surface in the same manner as observed experimentally. Then, we optimized the separation R of the 6-ring model with the rotational angle D fixed to reproduce the experimental observation. We list in Table 1 calculated heats of adsorption for the C_{60}−Cu_{10} systems, separations R's, and charges on the Cu_{10} cluster. Judging from the heats of adsorption, the strongest interaction is attained when a C_{60} molecule faces to the Cu_{10} cluster by a 6−6 bond. Coordination by an edge atom or a 5−6 bond also leads to a considerable amount of stabilization, whereas interaction by a 6- or a 5-ring is much weaker. Whether the rotational angle D is fixed or not, the 6-ring model has a large separation R and a small stabilization energy, and therefore appears not to be competitive. This is apparently in contrast to the XPD study on a C_{60}/Cu (111) monolayer,[1] which reported that C_{60} should adsorb on a Cu(111) surface by a 6-ring. The disagreement is most likely to be attributed to C_{60}−C_{60} interactions in the C_{60} monolayer systems. The models with large adsorption energies have small separations R's and large negative charges on the Cu_{10} part, which points to the importance of electron delocalization from C_{60} to Cu(111) surface. This is opposite to a general trend in organic systems (and alkali metal salts), where C_{60} plays a role as an electron acceptor. We demonstrate later that electron delocalization from the Cu(111) surface to C_{60} is weak in the single molecule adsorption of C_{60}.

Table 2 presents results of the B3LYP/LanL2MB calculations on larger C_{60}−Cu_{34} models. In contrast to the C_{60}−Cu_{10} models, the edge-atom model attains as strong a stabilizing interaction as the 6−6 bond model. This indicates that a C_{60} interacts with more Cu atoms in the edge-atom coordination than in the 6−6 bond coordination, as discussed later. Tables 1 and 2 show the same tendency, except for the heats of adsorption and electric charges of the edge-atom model. Thus, for the C_{60}−Cu_{34} models, the preference is in the order of edge atom $\approx$ 6−6 bond > 5−6 bond > 6-ring > 5-ring, being also different from the XPD result.[1]

The outcome of the B3LYP/LanL2MB calculations is consistent with the experimental observations for a single C_{60} molecule that the 6−6 bonds behave like olefinic unsaturated bonds in chemical reactions, e.g., adduct formation with transition metal complexes,[31] addition of electrophiles,[32] the

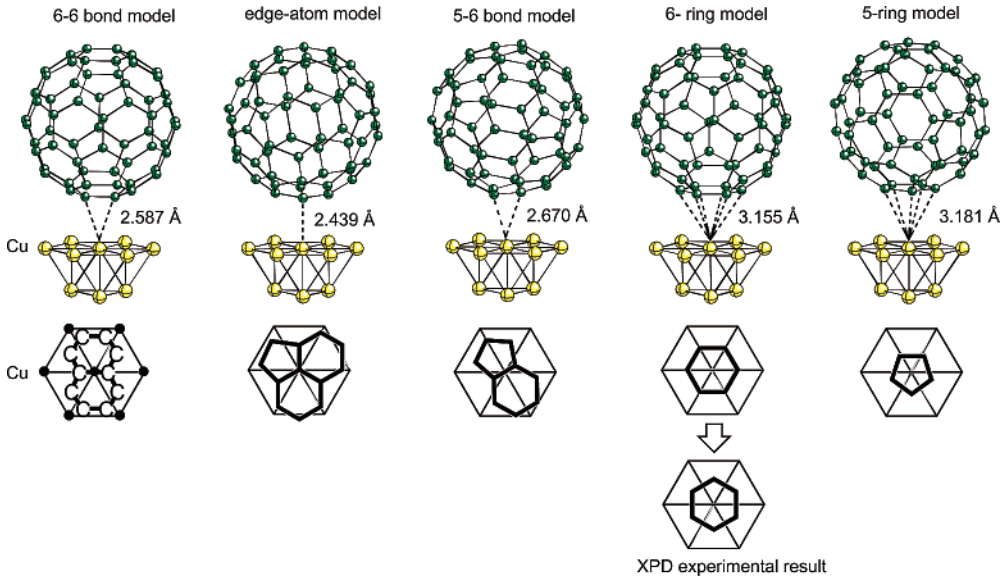

Figure 1. Optimized structures of the $C_{60}-Cu_{10}$ systems at the B3LYP/LanL2MB level of theory. An XPD result on C_{60}/Cu(111) monolayer is also shown.

TABLE 1: Results of B3LYP/LanL2MB Calculations on $C_{60}-Cu_{10}$ Systems

coordination mode	heat of adsorption[a]	separation R^b	charge on Cu_{10}[c]
6−6 bond	−1.935	6.022	−0.795
edge atom	−1.824	6.043	−0.743
5−6 bond	−1.763	6.093	−0.744
6-ring	−1.624	6.105	−0.637
6-ring[d]	−1.358	6.276	−0.563
5-ring	−1.436	6.300	−0.632

[a] Estimated by $[E(C_{60} + Cu_{10}) - E(C_{60}) - E(Cu_{10})]$ (in eV). [b] Distance between the center of gravity of the C_{60} sphere and the center Cu atom of the first layer of Cu_{10} (in Å). [c] Estimated by Mulliken population analysis. [d] Rotational angle D is fixed to be consistent with an XPD experimental result on a C_{60}/Cu(111) monolayer system.

TABLE 2: Results of B3LYP/LanL2MB Calculations on $C_{60}-Cu_{34}$ Systems

coordination mode	heat of adsorption[a]	separation R^b	charge on Cu_{34}[c]
6−6 bond	−3.010	6.022	−0.932
edge atom	−3.015	6.043	−0.949
5−6 bond	−2.795	6.093	−0.928
6-ring	−2.479	6.105	−0.889
5-ring	−2.447	6.300	−0.790

[a] Estimated by $[E(C_{60} + Cu_{34}) - E(C_{60}) - E(Cu_{34})]$ (in eV). [b] Distance between the center of gravity of the C_{60} sphere and the center Cu atom of the first layer of Cu_{34} (in Å). [c] Estimated by Mulliken population analysis.

Diels−Alder reaction with some dienes,[33] and dimerization reactions,[34] where five-membered and six-membered rings are inactive.

Copper is the only element of the first transition metal row where relativistic effects are important. We partially performed single-point calculations with the SDD basis set[35] to look at whether the relativistic effects of the Cu_{34} cluster affect the order of stability in these models. The 6−6 bond and edge-atom models are 0.363 and 0.323 eV more stable than the 6-ring model, respectively, at the B3LYP/SDD level of theory. The important order of stability is confirmed to be identical at the B3LYP/LanL2MB and SDD levels of theory.

PIO Analysis. Let us now look at the origin of $C_{60}-Cu(111)$ bonding by applying the paired-interaction-orbital (PIO) scheme[23] within the framework of the extended Hückel MO theory[36] to the $C_{60}-Cu_{34}$ models. As we will see, the PIO analysis agrees qualitatively with the energetics from B3LYP/LanL2MB calculations on the $C_{60}-Cu_{34}$ models. One will find that there is no key orbital interaction which should favor the single C_{60} adsorption by a 6-ring or a 5-ring.

Method of Analysis. To see what orbitals of C_{60} and the Cu(111) surface participate in C−Cu orbital interactions, we have carried out a PIO analysis on the $C_{60}-Cu_{34}$ models. The geometrical parameters around the reaction sites are identical to those optimized for the $C_{60}-Cu_{10}$ models. We have 187 occupied MOs and 119 unoccupied MOs for the Cu_{34} cluster and 120 occupied MOs and 120 unoccupied MOs for an adsorbed C_{60} molecule in the extended Hückel MO scheme. Delocalization of electrons between the two fragment systems occurs through combinations of the occupied MOs of one part and the unoccupied MOs of the other part.

Consider here an interaction between the occupied MO ϕ_i of one fragment, A, and the unoccupied MO ψ_l of the other fragment, B. The interaction gives rise to two orbitals of the composite system, A−B. Assuming that the occupied MO ϕ_i is located lower in energy than the MO ψ_l, as is often the case, the occupied MO of A−B is given by

$$\Phi_1 = c_i\phi_i + c_l\psi_l \text{ with } |c_i| > |c_l| \tag{1}$$

When the interaction between the two fragments is very weak, c_i and c_l are given by

$$c_i \cong 1 \tag{2}$$

$$c_l \cong \frac{H_{il} - S_{il}H_{il}}{H_{ii} - H_{ll}} \tag{3}$$

in which the integrals are defined for the Hamiltonian operator, H, of A−B

$$H_{ii} = \int \phi_i H \phi_i dv,\ H_{ll} = \int \psi_l H \psi_l dv,\ H_{il} = \int \phi_i H \psi_l dv$$

$$S_{il} = \int \phi_i \psi_l dv \tag{4}$$

The strength of interaction and the energy gap between the two

orbitals ϕ_i and ψ_l are represented by the numerator and the denominator of eq 3, respectively. The sign of the coefficient c_l in eq 1 depends on the sign of c_i. Thus, the product of two coefficients $c_i c_l$ can be a good measure of the mixing of the two MOs.

Each MO of the composite system A−B of two fragments is given in the extended Hückel MO calculation by a linear combination of the AOs of the two fragments. Then, the MO Φ_f of A−B can be rewritten in terms of a linear combination of the occupied and unoccupied MOs of the two fragment species, A and B

$$\Phi_f = \sum_{i=1}^{m} c_{fi}\phi_i + \sum_{j=m+1}^{M} c_{fj}\phi_j + \sum_{k=1}^{n} c_{fk}\psi_k + \sum_{l=n+1}^{N} c_{fl}\psi_l \quad (5)$$

where ϕ_i ($i = 1, 2, ..., m$) and ϕ_j ($j = m + 1, m + 2, ..., M$) denote respectively the occupied and unoccupied canonical MOs of the fragment A and ψ_k ($k = 1, 2, ..., n$) and ψ_l ($l = n + 1, n + 2, ..., N$) indicate respectively the occupied and unoccupied MOs of the fragment B. This is our fragment molecular orbital (FMO) scheme.[38] Now, we may regard P_{il} defined by eq 6 as the measure of interaction between the occupied MO ϕ_i of A and the unoccupied MO ψ_l of B in A−B[39]

$$P_{il} = 2\sum_{f=1}^{m+n} c_{fi}c_{fl} \quad (6)$$

Electron delocalization from C_{60} to the Cu_{34} cluster is represented by 120 × 119 orbital interactions. Now, let us carry out simultaneous transformations of the fragment MOs within the occupied MO space of the C_{60} part and within the unoccupied MO space of the Cu_{34} cluster, by diagonalizing $\mathbf{P}^\dagger\mathbf{P}$, the ($i$, l) element of $\mathbf{P}$ being P_{il}.[40] The purpose of doing this is to represent electron delocalization in terms of pairs of interaction orbitals ϕ_i' and ψ_l', the former being given by a linear combination of the occupied canonical MOs ϕ_i of C_{60} and the latter by a linear combination of the unoccupied canonical MOs ψ_l of the Cu_{34} cluster. As a consequence, we can reduce 120 × 119 orbital interactions to the interactions of 119 paired orbitals (ϕ_i'; ψ_l'), i, $l = f = 1 \sim 119$.[41] One will find shortly that the description of interactions is even simpler, being represented by still fewer orbital pairs. Delocalization of electrons from the Cu_{34} cluster to the C_{60} part is presented by 187 × 120 orbital interactions in the canonical MO scheme, but is dominated by several orbital pairs in our scheme.

The MOs of A−B are now represented in terms of transformed occupied and unoccupied orbitals of the two fragments, some of which participate in the bonding between the fragments by making orbital pairs and some of which do not contribute significantly to the bonding, being unpaired

$$\Phi_f = \sum_{i=1}^{m} d_{fi}\phi_i' + \sum_{j=m+1}^{M} d_{fj}\phi_j' + \sum_{k=1}^{n} d_{fk}\psi_k' + \sum_{l=n+1}^{N} d_{fl}\psi_l' \quad (7)$$

The contribution of each PIO to the change in energy ΔE is given by eq 8, when the interaction is not yet strong

$$\Delta E_{il} \cong \frac{2(H_{il}' - S_{il}'H_{ii}')^2}{H_{ii}' - H_{ll}'} \quad (8)$$

in which

$$H_{il}' = \int \phi_i' H \psi_l' d\upsilon,\ H_{ii}' = \int \phi_i' H \phi_i' d\upsilon,\ H_{ll}' = \int \psi_l' H \psi_l'\, d\upsilon$$

$$S_{il}' = \int \phi_i' \psi_l'\, d\upsilon \quad (9)$$

It turns out, however, that $|H_{il}' - S_{il}'H_{ii}'|$ is not very small, relative to $|H_{ii}' - H_{ll}'|$, in the systems under consideration. Then, ΔE_{il} may be evaluated by subtracting $2H_{ii}'$ from the twice of the lower eigenvalue of the following secular equations, to be used to estimate the magnitude of the contribution of each PIO to the C−Cu bonding in the following discussion:

$$\begin{vmatrix} H_{ii}' - \epsilon & H_{il}' - S_{il}'\epsilon \\ H_{il}' - S_{il}'\epsilon & H_{ll}' - \epsilon \end{vmatrix} = 0 \quad (10)$$

$|H_{il}' - S_{il}'H_{ii}'|$ and $|H_{ii}' - H_{ll}'|$ are still useful parameters in discussing the strength of electron delocalization, although we do not directly use eq 8 in this study.

Orbital Interactions between C_{60} and a Cu(111) Surface. Table 3 presents results on the three pairs of orbitals with the largest ΔE participating in delocalization of electrons from C_{60} to the Cu cluster, and from the latter to the former, for the five C_{60}−Cu_{34} models. For each model, we also list the total value of ΔE's over 119 orbital pairs and that over 120 pairs, which, respectively, represent the electron delocalization from C_{60} to Cu_{34} and that from Cu_{34} to C_{60}. Electron delocalization takes place predominantly from C_{60} to Cu_{34} in all of the five models, being consistent with the results of Mulliken population analysis at the B3LYP/LanL2MB level of theory (see Tables 1 and 2).

6−6 Bond Model. First let us look at orbital interactions in the 6−6 bond model. We present in Figure 2 the three pairs of interaction orbitals with the largest ΔE's that contribute to electron delocalization from the C_{60} part to the Cu_{34} part in the 6−6 bond model. The occupied orbital of C_{60} is shown above and the paired unoccupied orbital of Cu_{34} is given below in each pair. One finds that the orbitals have a large amplitude on the reaction sites but are delocalized over several carbon or Cu atoms around the reaction sites, indicating that the interactions between the two fragments are not weak, but also not very strong.

We illustrate in Scheme 3 the main part of the orbital pairs in Figure 2. In the first pair of orbitals, pair 1, an in-phase combination of two pπ-type AOs of the 6−6 bond overlaps in a bonding manner with a hybrid of dominant 4s and subsidiary 4p AOs of the central Cu atom of the first layer. This orbital interaction is strong, as shown by the large $|H_{il}' - S_{il}'H_{ii}'|$ and ΔE values. In pair 1, the extent of localization of the orbital ϕ_1' on the 6−6 bond is 69% and that of the orbital ψ_1' on the central Cu atom is 84%, according to the Mulliken population analysis at the extended Hückel level of theory. The contribution of the other Cu atoms in the first layer to ψ_1' is 10%, and the contributions of the second and third layers are very small. Thus, the interaction orbitals of pair 1 are well-localized on the reaction site, and the orbital interaction represented by pair 1 is quite effective. Pairs 2 and 3 show that the $2p_z$ orbitals of the other carbons of the two fused 6-rings of C_{60} also overlap in a bonding manner with the 4s orbitals of the neighboring Cu atoms, thus assisting the interaction at the main reaction site. The two orbital pairs look very similar to each other, but they are not degenerate. As seen in the smaller values of $|H_{il}' - S_{il}'H_{ii}'|$, the orbital overlaps in pairs 2 and 3 are less effective than that in pair 1, and therefore, contributions of these pairs to the C_{60}−Cu_{34} bonding are small (ΔE's are small). However, these weaker orbital interactions can make the 6−6 bond be parallel to one of the diagonal Cu−Cu−Cu bonds of the first-layer hexagon.

In Scheme 4, we illustrate the main part of the three orbital pairs with the largest ΔE's representing electron delocalization

TABLE 3: Stabilization Caused by Three Strongest Pairs of Interaction Orbitals (Namely the PIOs with the Largest Three ΔE's) (in eV)

coordination mode	$(H'_{il} - S'_{il}H'_{ii})^a$	$(H'_{ii} - H'_{ll})$	ΔE	sum of ΔEs over all pairs
edge atom				
from C_{60} to Cu_{34}				
pair 1	−0.936	−4.011	−0.391	
pair 2	−0.386	−3.873	−0.075	
pair 3	−0.347	−3.877	−0.061	−0.622[b]
from Cu_{34} to C_{60}				
pair 1	−0.532	−4.199	−0.131	
pair 2	−0.608	−7.390	−0.099	
pair 3	−0.278	−3.050	−0.050	−0.355[c]
6−6 bond				
from C_{60} to Cu_{34}				
pair 1	−0.938	−3.903	−0.402	
pair 2	−0.269	−1.775	−0.079	
pair 3	−0.346	−3.896	−0.060	−0.641[b]
from Cu_{34} to C_{60}				
pair 1	−0.420	−2.876	−0.119	
pair 2	−0.732	−11.976	−0.089	
pair 3	−0.246	−3.100	−0.039	−0.305[c]
5−6 bond				
from C_{60} to Cu_{34}				
pair 1	−0.743	−3.776	−0.270	
pair 2	−0.314	−2.109	−0.090	
pair 3	−0.280	−2.553	−0.060	−0.519[b]
from Cu_{34} to C_{60}				
pair 1	−0.480	−5.643	−0.081	
pair 2	−0.370	−4.083	−0.066	
pair 3	−0.347	−5.196	−0.046	−0.245[c]
6-ring				
from C_{60} to Cu_{34}				
pair 1	−0.264	−1.567	−0.086	
pair 2	−0.264	−1.567	−0.086	
pair 3	−0.360	−4.366	−0.058	−0.353[b]
from Cu_{34} to C_{60}				
pair 1	−0.276	−3.363	−0.045	
pair 2	−0.276	−3.363	−0.045	
pair 3	−0.428	−10.261	−0.036	−0.195[c]
5-ring				
from C_{60} to Cu_{34}				
pair 1	−0.175	−1.738	−0.035	
pair 2	−0.181	−1.858	−0.035	
pair 3	−0.302	−4.661	−0.039	−0.162[b]
from Cu_{34} to C_{60}				
pair 1	−0.213	−2.491	−0.036	
pair 2	−0.213	−2.531	−0.035	
pair 3	−0.345	−8.512	−0.028	−0.122[c]

[a] S'_{il} is taken to be positive. [b] Sum over 119 pairs. [c] Sum over 120 pairs.

from the Cu_{34} cluster to C_{60} in the 6−6 bond model; the occupied orbital of Cu_{34} is shown below and the paired unoccupied orbital of C_{60} is given above. Pair 1 indicates that electric charge is transferred from the $3d_{xz}$ AO of the central Cu atom of the first layer to the out-of-phase combination of the two $2p_z$ AOs of the 6−6 bond. However, the orbital interaction by this pair is much weaker than that in pair 1 of Figure 2 (Scheme 3). In pair 2, the $3d_{z^2}$ orbital of the central Cu atom overlaps mainly with the in-phase combination of the two $2p_z$ orbitals of the 6−6 bond in a bonding manner, involving small antibonding interactions with the $2p_z$ orbitals of the C atoms adjacent to the 6−6 bond. Pair 3 shows that $2p_z$ orbitals of the C atoms around the main reaction site interact in-phase with the 4s orbitals of the neighboring Cu atoms. Orbital interactions in pairs 2 and 3 are not effective, either. In total, orbital interactions showing electron delocalization from the Cu_{34} part are not strong, compared to those representing electron delocalization from the C_{60} part. This is the reason electrons are transferred from the Cu cluster to C_{60}.

Edge-Atom Model. Schemes 5 and 6 illustrate three important orbital pairs that contribute to electron delocalization from C_{60} to Cu_{34} and from Cu_{34} to C_{60} in the edge-atom model. The C_{60} molecule interacts with the Cu_{34} cluster not only through an edge carbon atom but also through several surrounding carbons. The coordination through an edge carbon atom bears a resemblance to that by a 6−6 bond, in that bonding overlap between the in-phase combination of $2p_z$ AOs of a 6−6 bond and the 4s AO of the central Cu atom plays the most important role (pair 1 in Scheme 5). The out-of-phase combination of the $2p_z$ AOs of the 6−6 bond (pair 1 of Scheme 6), which is similar to pair 1 in Scheme 4, is also important. However, stabilization caused by pair 1 of Scheme 6 (−0.131 eV) is much smaller than that by pair 1 of Scheme 5 (−0.391 eV), being similar to the case of the 6−6 bond model. This tells us that electron delocalization takes place from C_{60} to Cu_{34} also in the edge-atom model.

It is interesting that a 6−6 bond mainly interacts with the Cu_{34} cluster in the edge-atom model. Being similar to the 6−6 bond model, the $2p_z$ AOs of other carbon atoms of the two fused 6-rings contribute significantly to orbital interactions in pairs 2 and 3 in the edge-atom model. The interaction orbitals are not localized at the interaction center as significantly as in the 6−6 bond model. Localization of orbital ϕ'_1 on the 6−6 bond is 60% and that of orbital ψ'_1 on the central Cu atom is 81% in pair 1 of Scheme 5, being smaller than those for pair 1 of Figure 2 (Scheme 3) (69% and 84%, respectively). This is a part of the reason that electron delocalization from the C_{60} part (represented by the first three pairs) is slightly weaker than that in the 6−6 bond model; the sum of ΔE over pair 1 ∼ pair 3 is −0.527 eV in the edge-atom model, being smaller than −0.541 eV for the 6−6 bond model. The sum of ΔE over 119 orbital pairs (−0.622 eV) is also slightly smaller than that of the 6−6 bond model (−0.641 eV).

On the other hand, ΔE's over 120 orbital pairs add up to −0.355 eV, being larger than that of the 6−6 bond model (−0.305 eV). Therefore, electron delocalization from the Cu_{34} cluster is stronger in the edge-atom model than in the 6−6 bond model. In total, the sum of ΔE over 239 (119 + 120) interactions (−0.977 eV) slightly exceeds that in the 6−6 bond model (−0.946 eV). Thus, C_{60} is considered to interact slightly better through an edge atom with a Cu(111) surface. These results are in line with those obtained by the B3LYP/LanL2MB calculations on the C_{60}−Cu_{34} systems, which give a slightly lower energy and slightly larger negative charge on the Cu_{34} cluster for the edge-atom model.

5−6 Bond Model. The coordination by a 5−6 bond is less favored. The first pair representing electron delocalization from C_{60} to Cu_{34} is dominant, as in the 6−6 bond and edge-atom models. The in-phase combination of the $2p_z$ AOs on a 5−6 bond overlaps in-phase with the 4s AO of the central Cu atom in the first pair, as shown in Scheme 7. The shape of the first pair resembles those of the corresponding first pairs in the 6−6 bond model and edge-atom model, although the key pπ orbital is on a 5−6 bond in this case, whereas those of the preferred two models are on 6−6 bonds. However, ΔE for the first pair (−0.270 eV) of the 5−6 bond model is small compared to the corresponding ΔE's in the two favored models (−0.402 and −0.391 eV). Some neighboring atoms assist the interaction at the reaction center, but the subsidiary interactions are weak. Electron transfer occurs from C_{60} to Cu_{34}, as expected. Thus, coordination of C_{60} by a 5−6 bond is less likely, if not negligible.

6-Ring Model. Pairs 1 and 2 of Scheme 8 show that two occupied orbitals of C_{60}, resembling the degenerate HOMOs of benzene, interact with the 4s AOs of several Cu atoms. These

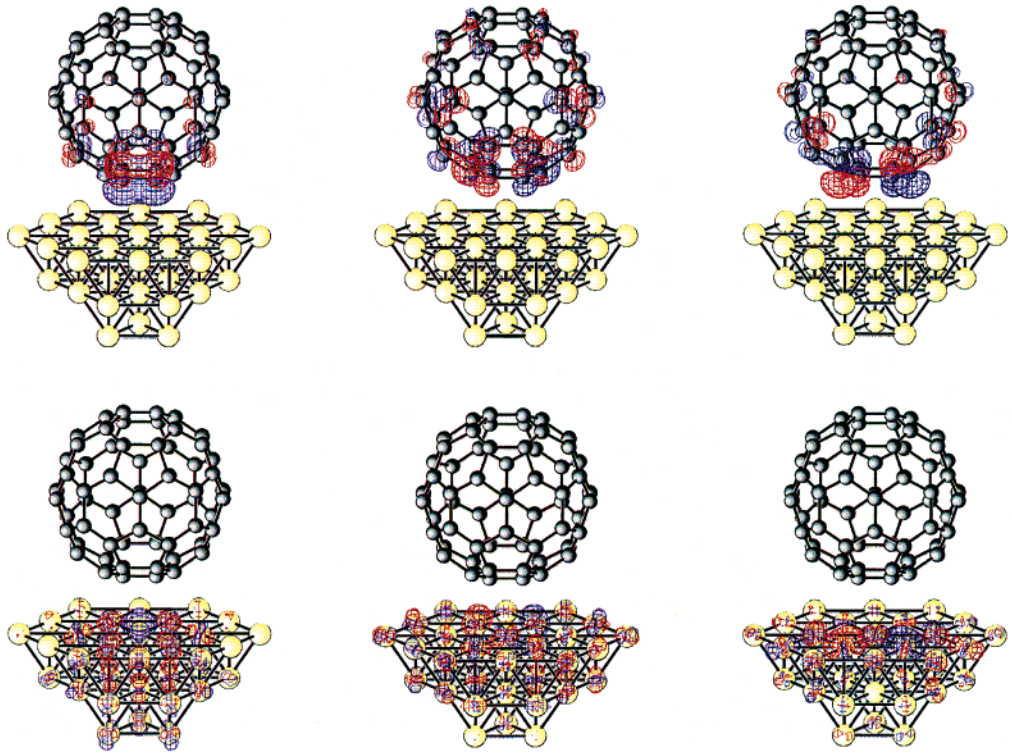

Figure 2. Three strongest pairs of interaction orbitals representing electron delocalization from the C_{60} part to the Cu_{34} cluster part in the 6−6 bond model. Orbital ϕ' indicates the occupied interaction orbital of C_{60}, and ψ' denotes the unoccupied interaction orbital of the Cu cluster in each pair.

SCHEME 3

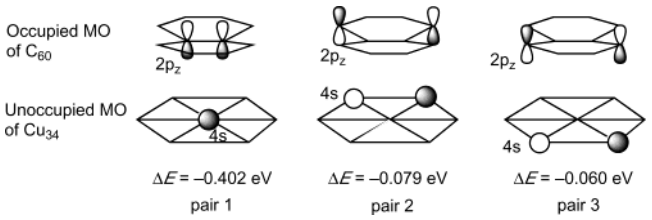

SCHEME 4

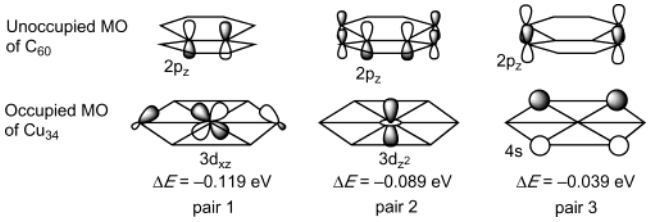

SCHEME 5

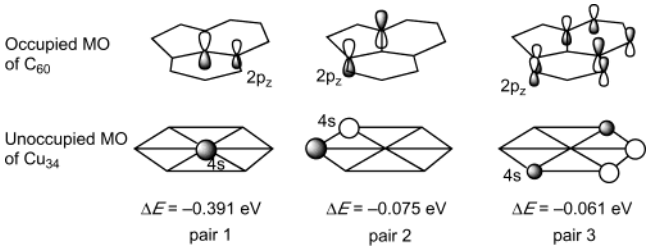

SCHEME 6

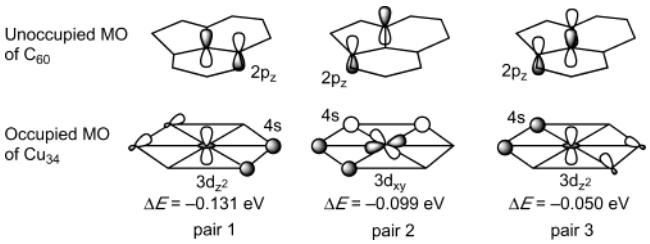

SCHEME 7

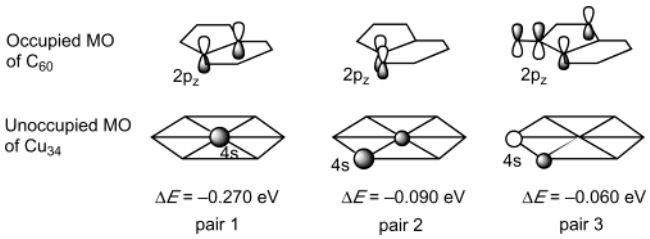

SCHEME 8

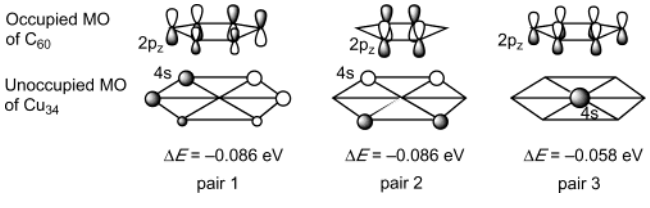

pairs of orbitals do not have effective bonding overlap between the two fragments, as demonstrated by the small $|H'_{il} - S'_{il}H'_{ii}|$ and ΔE values. Note that these two pairs are degenerate in the system under consideration. In pair 3 of Scheme 8, the occupied orbital of C_{60} that looks like the lowest lying π MO of benzene interacts with the 4s AO of the central Cu atom, but ΔE is small (−0.058 eV). The reason is that the occupied C_{60} orbital of pair 3 has strong bonding character and low energy and, consequently, leads to a large $|H'_{ii} - H'_{ll}|$ value (−4.366 eV) compared to those of pairs 1 and 2. Electron delocalization from the Cu cluster to the C_{60} fragment is ineffective and charge transfer takes place from C_{60} to Cu_{34}. The C−Cu bonding in the 6-ring model is weaker than that in the 5−6 bond model.

5-Ring Model. In the 5-ring model, interaction orbitals of C_{60} look like π MOs of cyclopentadiene, which interact mainly with the 4s AOs of Cu_{34}. Matching of the orbital phase in each orbital pair is worse than that in the 6-ring model, and delocalization of electrons between the interaction orbitals is more difficult. Coordination by a 5-ring is least favored among the five models.

The PIO results are totally consistent with the B3LYP/LanL2MB calculations in energies and electronic charges shifted from the C_{60} part to the Cu_{34} part. According to our calculations, preference for the adsorption mode of a single C_{60} molecule to the three-layer Cu_{34} cluster is in the following order: edge atom $\approx$ 6−6 bond > 5−6 bond > 6-ring > 5-ring. The $2p_z$ AOs on a 6−6 bond of C_{60} and the 4s AO of the central Cu atom of the first layer play very important roles in the C_{60}−Cu_{34} bonding in the 6−6 bond model and the edge-atom model, whereas there is no key orbital interaction that strongly stabilizes coordination by a 6-ring or a 5-ring.

Conclusions

Using a two-layer Cu_{10} cluster and a three-layer Cu_{34} cluster as models of a Cu(111) surface, we have investigated the adsorption of a single C_{60} molecule onto a Cu(111) surface in terms of energetics and orbital interactions. Our B3LYP/LanL2MB calculations show that a single C_{60} molecule should contact a Cu(111) surface preferably by an edge carbon atom located at the center of two six-membered and one five-membered fused rings or by a C−C bond jointing two six-membered rings (6−6 bond). A paired-interaction-orbital (PIO) analysis in the extended Hückel MO scheme yields results consistent with the B3LYP/LanL2MB calculations. In coordination by a 6−6 bond, electron delocalization takes place efficiently from the occupied $2p\pi$ orbital localized on a 6−6 bond to the unoccupied 4s orbital of the Cu atom located beneath the midpoint of the 6−6 bond. In edge-atom coordination, the interaction orbitals are not significantly localized, and a greater number of carbon atoms participate in the interaction with the Cu_{34} cluster, whereas the shapes of important interaction orbitals are similar to those of the 6−6 bond coordination. This mode of coordination is slightly more favored than coordination by a 6−6 bond. Electron delocalization from the Cu_{34} cluster is not efficient in every case studied, and C_{60} should act as an electron donor, unlike its role in other organic reactions. No key orbital interaction that favors coordination by a six-membered ring or a five-membered ring has been found. These results do not agree with an XPD result for a C_{60} monolayer on Cu(111) where C_{60} molecules were suggested to bond to Cu(111) through a six-membered ring. The disagreement indicates that C_{60}−C_{60} interactions are also important to determine C_{60} orientations on solid surfaces.

Acknowledgment. K.Y. acknowledges the Ministry of Culture, Sports, Science and Technology of Japan and the Japan Society for the Promotion of Science, and the Murata Science Foundation for their support of this work. A part of this work was supported by Kyushu University P & P "Green Chemistry". Computations were in part carried out at the Computer Center of the Institute for Molecular Science. We thank Professor Shigeyoshi Sakaki of Kyoto University for computational assistance. A.O. and M.K. thank the Japan Society for the Promotion of Science for graduate fellowships. The work at Cornell was supported by the National Science Foundation through Grant CHE02-04841.

References and Notes

(1) Fasel, R.; Aebi, P.; Agostino, R. G.; Naumovi'c, D.; Osterwalder, J.; Santaniello, A.; Schlapbach, L. *Phys. Rev. Lett.* **1996**, *76*, 4733.

(2) Murray, P. W.; Pedersen, M. Ø.; Lægsgaard, E.; Stensgaard, I.; Besenbacher, F. *Phys. Rev. B* **1997**, *55*, 9360.

(3) Fasel, R.; Agostino, R. G.; Aebi, P.; Schlapbach, L. *Phys. Rev. B* **1999**, *60*, 4517.

(4) Cepek, C.; Goldoni, A.; Modesti, S. *Phys. Rev. B* **1996**, *53*, 7466.

(5) Pedio, M.; Hevesi, K.; Zema, N.; Capozi, M.; Perfetti, P.; Gouttebaron, R.; Pireaux, J.-J.; Caudano, R.; Rudolf, P. *Surf. Sci.* **1999**, *437*, 249.

(6) Hunt, M. R. C.; Modesti, S.; Rudolf, P.; Palmer, R. E. *Phys. Rev. B* **1995**, *51*, 10039.

(7) Modesti, S.; Cerasari, S.; Rudolf, P. *Phys. Rev. Lett.* **1993**, *71*, 2469.

(8) Maxwell, A. J.; Brühwiler, P. A.; Nilsson, A.; Mårtensson, N.; Rudolf, P. *Phys. Rev. B* **1994**, *49*, 10717.

(9) Pedio, M.; Felici, R.; Torrelles, X.; Rudolf, P.; Capozi, M.; Rius, J.; Ferrer, S. *Phys. Rev. Lett.* **2000**, *85*, 1040.

(10) Weckesser, J.; Barth, J. V.; Kern, K. *Phys. Rev. B* **2001**, *64*, 161403(R).

(11) Weckesser, J.; Cepek, C.; Fasel, R.; Barth, J. V.; Baumberger, F.; Greber, T.; Kern, K. *J. Chem. Phys.* **2001**, *115*, 9001.

(12) Giudice, E.; Magnano, E.; Rusponi, S.; Boragno, C.; Valbusa, U. *Surf. Sci.* **1998**, *405*, L561.

(13) Cepek, C.; Fasel, R.; Sancrotti, M.; Greber, T.; Osterwalder, J. *Phys. Rev. B* **2001**, *63*, 125406.

(14) Klyachko, D.; Chen, D. M. *Phys. Rev. Lett.* **1995**, *75*, 3693.

(15) Hou, J. G.; Jinlong, Y.; Haiqian, W.; Qunxiang, L.; Changgan, Z.; Hai, L.; Wang, B.; Chen, D. M.; Qingshi, Z. *Phys. Rev. Lett.* **1999**, *83*, 3001.

(16) Pascual, J. I.; Gómez-Herrero, J.; Rogero, C.; Baró, A. M.; Sánchez-Portal, D.; Artacho, E.; Ordejón, P.; Soler, J. M. *Chem. Phys. Lett.* **2000**, *321*, 78.

(17) Girifalco, L. A.; Hodak, M.; Lee, R. S. *Phys. Rev. B* **2000**, *62*, 13104.

(18) Nakamura, J.; Nakayama, T.; Watanabe, S.; Aono, M. *Phys. Rev. Lett.* **2001**, *87*, 48301.

(19) C_{60}−Cu interactions in the C_{60}/Cu composite films have been studied experimentally: Hou, J. G.; Li, X.; Wang, H.; Wang, B. *J. Phys. Chem. Solids* **2000**, *61*, 995.

(20) (a) Sakurai, T.; Wang, X. D.; Hashizume, T.; Yurov, V.; Shinohara, H.; Pickering, H. W. *Appl. Surf. Sci.* **1995**, *87/88*, 405. (b) Fartash, A. *J. Appl. Phys.* **1996**, *79*, 742. (c) Tsuei, K.-D.; Johnson, P. D. *Solid State Commun.* **1997**, *101*, 337. (d) Dutton, G.; Zhu, X.-Y. *J. Phys. Chem. B* **2002**, *106*, 5975. (e) Silien, C.; Marenne, I.; Auerhammer, J.; Tagmatarchis, N.; Prassides, K.; Thiry, P. A.; Rudolf, P. *Surf. Sci.* **2001**, *482*−*485*, 1.

(21) Tang, H.; Cuberes, M. T.; Joachim, C.; Gimzewski, J. K. *Surf. Sci.* **1997**, *386*, 115.

(22) Fujimoto, H.; Nakao, Y.; Fukui, K. *J. Mol. Struct.* **1993**, *300*, 425.

(23) Tachibana, M. Yoshizawa, K.; Ogawa, A.; Fujimoto, H.; Hoffmann, R. *J. Phys. Chem. B* **2002**, *106*, 12727.

(24) Experimental results (ref 1) indicate that C_{60} adsorbed at the *on-top* site is most stable.

(25) (a) Becke, A. D. *J. Chem. Phys.* **1993**, *98*, 5648. (b) Becke, A. D.; Roussel, M. R. *Phys. Rev. A* **1989**, *39*, 3761. (c) Lee, C.; Yang, W.; Parr, R. G. *Phys. Rev. B* **1988**, *37*, 785. (d) Stephens, P. J.; Devlin, F. J.; Chabalowski, C. F.; Frisch, M. J. *J. Phys. Chem.* **1994**, *98*, 11623.

(26) (a) Hehre, W. J.; Stewart, R. F.; Pople, J. A. *J. Chem. Phys.* **1969**, *51*, 2657. (b) Collins, J. B.; Schleyer, P. v. R.; Binkley, J. S.; Pople, J. A. *J. Chem. Phys.* **1976**, *64*, 5142. (c) Hay, P. J.; Wadt, W. R. *J. Chem. Phys.* **1985**, *82*, 299.

(27) Frisch, M. J.; Trucks, G. W.; Schlegel, H. B.; Scuseria, G. E.; Robb, M. A.; Cheeseman, J. R.; Zakrzewski, V. G.; Montgomery, J. A., Jr.; Stratmann, R. E.; Burant, J. C.; Dapprich, S.; Millam, J. M.; Daniels, A. D.; Kudin, K. N.; Strain, M. C.; Farkas, O.; Tomasi, J.; Barone, V.; Cossi, M.; Cammi, R.; Mennucci, B.; Pomelli, C.; Adamo, C.; Clifford, S.; Ochterski, J.; Petersson, G. A.; Ayala, P. Y.; Cui, Q.; Morokuma, K.; Malick, D. K.; Rabuck, A. D.; Raghavachari, K.; Foresman, J. B.; Cioslowski, J.; Ortiz, J. V.; Stefanov, B. B.; Liu, G.; Liashenko, A.; Piskorz, P.; Komaromi, I.; Gomperts, R.; Martin, R. L.; Fox, D. J.; Keith, T.; Al-Laham, M. A.; Peng, C. Y.; Nanayakkara, A.; Gonzalez, C.; Challacombe, M.; Gill, P. M. W.; Johnson, B. G.; Chen, W.; Wong, M. W.; Andres, J. L.; Head-Gordon, M.; Replogle, E. S.; Pople, J. A. *Gaussian 98*, revision A.7; Gaussian, Inc.: Pittsburgh, PA, 1998.

(28) Johnson, R. D.; Yannoni, N.; Meijer, G.; Bethune, D. S. in *The MRS Late News Session-Buckyballs: New Materials Made from Carbon Soot*(videotape); Materials Research Society: Pittsburgh, PA, 1990.

(29) (a) Yannoni, C. S.; Bernier, P. P.; Bethune, D. S.; Meijer, G.; Salem, J. R. *J. Am. Chem. Soc.* **1991**, *113*, 3190. (b) Fleming, R. M.; Siegrist, T.; Marsh, P. M.; Hessen, B.; Kortan, A. R.; Murphy, D. W.; Haddon, R. C.; Tycko, R.; Dabbagh, G.; Mujsce, A. M.; Kaplan, M. L.; Zahurak, S. M. *Mater. Res. Soc. Symp. Proc.* **1991**, *206*, 691.

(30) It is suggested that deformation of C_{60} on attachment to a Cu(111) surface is very small, because this interactions are very weak compared to C−C covalent bonds.

(31) (a) Fagan, P. J.; Calabrese, J. C.; Malone, B. *Acc. Chem. Res.* **1992**, *25*, 5, 134. (b) Nunzi, F.; Sgamellotti, A.; Re, N.; Floriani, C. *Organometallics* **2000**, *19*, 1628.

(32) Kitagawa, T.; Sakamoto, H.; Takeuchi, K. *J. Am. Chem. Soc.* **1999**, *121*, 4298.

(33) (a) Komatsu, K.; Murata, Y.; Sugita, N.; Takeuchi, K.; Wan, T. S. M. *Tetrahedron Lett.* **1993**, *34*, 8473. (b) Ishida, H.; Komori, K.; Itoh, K.; Ohno, M. *Tetrahedron Lett.* **2000**, *41*, 9839.

(34) (a) Strout, D. L.; Murry, R. L.; Xu, C.; Eckhoff, W. C.; Odom, G. K.; Scuseria, G. E. *Chem. Phys. Lett.* **1993**, *214*, 576. (b) Halevi, E. A. *Helv. Chim. Acta* **2001**, *84*, 1661.

(35) (a) Andrae, D.; Haeussermann, U.; Dolg, M.; Stoll, H.; Preuss, H. *Theor. Chim. Acta* **1990**, *77*, 123. (b) Bergner, A.; Dolg, M.; Kuechle, W.; Stoll, H.; Preuss, H. *Mol. Phys.* **1993**, *80*, 1431. (c) Dolg, M.; Wedig, U.; Stoll, H.; Preuss, H. *J. Chem. Phys.* **1987**, *86*, 866. (d) Dunning, T. H., Jr.; Hay, P. J. In *Modern Theoretical Chemistry*; Schaefer, H. F., III., Ed.; Plenum: New York, 1976; Vol. 3, p 1.

(36) (a) Hoffmann, R.; Lipscomb, W. N. *J. Chem. Phys.* **1962**, *36*, 2179; *37*, 2872. (b) Hoffmann, R. *J. Chem. Phys.* **1963**, *39*, 1397. (c) Hoffmann, R. *J. Chem. Phys.* **1964**, *40*, 2474, 2745.; the extended Hückel calculation and MO drawing are perfomed using the YAeHMOP program.[37]

(37) Landrum, G. A.; Glassey, W. V. *YAeHMOP: Yet Another extended Hückel Molecular Orbital Package*; Cornell University: Ithaca, New York, 1995. http://sourceforge.net/projects/yaehmop/.

(38) Fujimoto, H.; Hoffmann, R. *J. Phys. Chem.* **1974**, *78*, 1167.

(39) Other orbital effects, e.g., polarization, are also included in the coefficients.

(40) (a) Fujimoto, H.; Koga, N.; Fukui, K. *J. Am. Chem. Soc.* **1981**, *103*, 7452. (b) Fujimoto, H.; Yamasaki, T.; Mizutani, H.; Koga, N. *J. Am. Chem. Soc.* **1985**, *107*, 6157. (c) Fujimoto, H.; Yamasaki, T. *J. Am. Chem. Soc.* **1986**, *108*, 578. (d) Omoto, K.; Sawada, Y.; Fujimoto, H. *J. Am. Chem. Soc.* **1996**, *118*, 1750. (e) Omoto, K.; Fujimoto, H. *J. Am. Chem. Soc.* **1997**, *119*, 5366.

(41) From here on, the prime denotes the transformed orbitals and the quantities defined for those orbitals.